Antiapoptotic Activity of Autocrine Interleukin-22 and Therapeutic Effects of Interleukin-22-Small Interfering RNA on Human Lung Cancer Xenografts

Weici Zhang,[1] Yongyan Chen,[1] Haiming Wei,[1] Chaogu Zheng,[1] Rui Sun,[1] Jian Zhang,[2] and Zhigang Tian[1,2]

Abstract

Purpose: Non – small cell lung carcinoma (NSCLC) is one of most common malignant diseases and usually is resistant against apoptosis-inducing chemotherapy. This study is to explore the antiapoptotic mechanisms of interleukin (IL)-22 in human lung cancer.

Experimental Design: Nineteen cases with stage I to III NSCLC were collected to determine the expression of IL-22. Stable transfection of human IL-22 cDNA into A549 and PG cells and transfection of IL-22-RNA interference (RNAi) into these cancer cell lines were done to reveal the molecular mechanisms of IL-22.

Results: It was found that IL-22 was highly expressed in primary tumor tissue, malignant pleural effusion, and serum of patients with NSCLC. IL-22R1 mRNA was also detected in lung cancer tissues as well as lung cancer cell lines. Overexpression of IL-22 protected lung cancer cell lines from serum starvation-induced and chemotherapeutic drug-induced apoptosis via activation of STAT3 and its downstream antiapoptotic proteins such as Bcl-2 and Bcl-xL and inactivation of extracellular signal-regulated kinase 1/2. Exposure to blocking antibodies against IL-22R1 or transfection with the IL-22-RNAi plasmid *in vitro* resulted in apoptosis of these lung cancer cells via STAT3 and extracellular signal-regulated kinase 1/2 pathways. Furthermore, an *in vivo* xenograft study showed that administration of IL-22-RNAi plasmids significantly inhibited the human tumor cell growth in BALB/c nude mice.

Conclusions: Our study indicates that autocrine production of IL-22 contributes to human lung cancer cell survival and resistance to chemotherapy through the up-regulation of antiapoptotic proteins.

Lung cancer is the third most common malignant disease and about 75% of all diagnosed lung cancers are the non-small cell lung carcinoma (NSCLC), which is associated with very dismal prognoses. Chemotherapy in addition to surgical resection and radiotherapy remains a basic strategy for treatment of malignant tumors. Unfortunately, NSCLC exhibits only limited sensitivity to chemotherapeutic drugs, which has proven to be a major obstacle clinically. Inhibition of cell apoptotic pathways was reported as one important cellular mechanism responsible for the resistance of NSCLC cells to treatments (1–4).

Interleukin (IL)-22 is one of the IL-10-related cytokines (5, 6). The functional IL-22 receptor complex consists of two chains, IL-22R1 and IL-10R2, which are ubiquitously expressed in various of organs and cell types including immune cells, lung, liver, and colon (7, 8). In response to IL-22 in the liver, rapid STAT phosphorylation and/or activation of Akt were observed (9) and contributed to improving hepatocyte survival (10, 11) and proliferation (12). IL-22 expression has been found in alveolar macrophages and alveolar epithelial cells isolated from bronchoalveolar lavage fluid and normal lung sections (13). Lower levels of IL-22 were detected in the bronchoalveolar lavage fluid from patients with pulmonary sarcoidosis and acute respiratory distress syndrome than normal control groups (13). Although these observations suggest involvement of IL-22 in the regulation of pulmonary inflammation, the potential role of IL-22 in the cell survival of lung cancer has not been explained thus far.

In this study, high expression levels of IL-22 were detected in primary tumor tissue, malignant pleural effusion, and serum of patients with NSCLC. Additionally, both IL-22R1 and IL-22 were highly expressed in primary lung cancer. Overexpression of IL-22 by gene transfer protected lung cancer cells from

Authors' Affiliations: [1]Institute of Immunology, Hefei National Laboratory for Physical Sciences at Microscale and School of Life Sciences, University of Science and Technology of China, Hefei, People's Republic of China and [2]Institute of Immunopharmacology and Immunotherapy, School of Pharmaceutical Sciences, Shandong University, Jinan, People's Republic of China

Received 9/20/07; revised 5/11/08; accepted 5/15/08.

Grant support: Natural Science Foundation of China grants 30630059, 30671901, 30570819, and 30571695 and Ministry of Science and Technology of China (973 Basic Science Project grants 2006CB504300, 2006CB806504, 2004CB518807, and 2003CB515501).

The costs of publication of this article were defrayed in part by the payment of page charges. This article must therefore be hereby marked *advertisement* in accordance with 18 U.S.C. Section 1734 solely to indicate this fact.

Note: Supplementary data for this article are available at Clinical Cancer Research Online (http://clincancerres.aacrjournals.org/).

W. Zhang and Y. Chen equally contributed to this study.

Requests for reprints: Zhigang Tian, School of Life Sciences, University of Science and Technology of China, 443 Huangshan Road, Hefei, Anhui 230027, People's Republic of China. Phone: 86-551-360-7379; Fax: 86-551-360-6783; E-mail: tzg@ustc.edu.cn.

doi:10.1158/1078-0432.CCR-07-4401

Translational Relevance

The limited sensitivity of non-small cell lung carcinoma (NSCLC) to chemotherapeutic drugs is a key barrier to the treatment of this malignant disease. This study has revealed a mechanism that NSCLC cells are able to escape chemotherapy-induced apoptosis through the interleukin (IL)-22 pathway. IL-22 expression levels are significantly elevated in primary tumor tissue, malignant pleural effusion, and serum of patients with NSCLC. This may allow for the improved diagnostic as well as prognostic evaluations based on the level of IL-22 expression. Our study shows that the autocrine production of IL-22 by lung cancer cell lines prevents apoptosis and promotes their resistance to chemotherapeutic drugs. Due to the recent advances in RNA interference (RNAi) silencing, we are able to inhibit IL-22 expression in both lung cancer cell lines and BALB/c nude mice xenografted with human tumor cells by using IL-22 RNAi plasmids. The administration of IL-22 RNAi plasmids significantly enhances apoptosis and then increases the chemotherapeutic sensitivity in lung cancer cell lines and finally inhibits human tumor cell growth in the mice. Therefore, the blockade of IL-22 signaling by antibodies and RNAi against IL-22 or IL-22R, in conjunction with conventional cancer treatments, may prove to be a potential therapeutic intervention for human NSCLC and need to be further investigated.

apoptosis via activation of STAT3 and its downstream antiapoptotic proteins and inactivation of extracellular signal-regulated kinase (ERK) 1/2. Treatment with IL-22R1 blocking antibodies or IL-22-RNA interference (RNAi) *in vitro* resulted in the apoptosis of lung cancer cells. Administration of IL-22-RNAi plasmids also significantly inhibited the growth of human lung cancer cell in BALB/c nude mice.

Materials and Methods

Chemicals, protein, and antibodies. 5-Fluorouracil (5-FU; Shanghai Xudong Haipu Pharmaceutical Co.) and carboplatin (Shandong Qilu Pharmaceutical Co.), two types of chemotherapeutic drugs, were used in our study. Recombinant human IL-22 was purchased from R&D Systems. The following primary antibodies were used in this study: goat anti-human IL-22 antibodies (R&D Systems), goat anti-human IL-22R1 blocking antibodies (R&D Systems), anti-phosphorylated STAT3 antibodies (Tyr^{705}; Ser^{727}), anti-STAT3 antibodies, anti-Bcl-2 antibodies, anti-Bcl-xL antibodies, anti-phosphorylated ERK1/2 antibodies (Thr^{202}/Tyr^{204}), anti-ERK1/2 antibodies, anti-phosphorylated AKT antibodies (Ser^{473}), anti-AKT antibodies (Cell Signaling Technology), and β-actin (Santa Cruz Biotechnology). Secondary antibodies that were used in this study: peroxidase-conjugated affinity-purified anti-goat IgG (Rockland) and peroxidase-conjugated affinity-purified anti-rabbit IgG (Sigma). All antibodies used in our study are polyclonal antibodies.

Cell culture. All cell lines were cultured at 37°C in 5% CO_2-95% air in the following medium supplemented with 10% heat-inactivated fetal bovine serum, 100 units/mL penicillin, and 100 μg/mL streptomycin. PG (large cell lung cancer cell line) and A549 (lung adenocarcinoma cell line) cells and their IL-22 or mock plasmid-transfected cells in RPMI 1640 (Invitrogen); H460, H1299, 95D, and HEK293 cell lines in DMEM (Invitrogen); SK-LU-1 and SK-MES-1 cell lines in MEM (Invitrogen) with 0.1 mmol/L nonessential amino acids, 2 mmol/L L-glutamine, and 1.0 mmol/L sodium pyruvate; and HUV-EC-C cells were in F-12 (Invitrogen).

Specimens and immunohistochemistry. Nineteen cases with stage I to III NSCLC were collected from the Second Affiliated Hospital of Hebei Medical University between January 2004 and July 2007. Immunohistochemical assays were done on 5 μm formalin-fixed, paraffin-embedded sections. Briefly, deparaffinized sections were microwaved for 10 min in 10 mmol/L citrate buffer (pH 6.0) for antigen retrieval. The slides were blocked against endogenous peroxidase activity by 1.5% hydrogen peroxide solution for 20 min and were incubated with polyclonal anti-human IL-22 antibody at 4°C overnight. After washing with TBS (pH 7.6), slides were treated with biotinylated anti-goat immunoglobulins, washed in TBS, and incubated in streptavidin peroxidase. Staining was visualized with 3,3′-diaminobenzidine tetrahydrochloride (Sigma) as a chromogen. Counterstaining of cells and tissue sections was done using hematoxylin.

Stable transfection of human IL-22 cDNA into A549 and PG cells. A549 and PG cells were seeded in six-well culture plates and transfected with pcDNA3-IL-22 plasmid using LipofectAMINE 2000 (Invitrogen) in a 90% to 95% cell confluent state. Stably transfected cell lines derived from the single-cell clone were obtained after selective scanning by G418 (800-1,000 μg/mL; Life Technologies) and limiting dilution culture. IL-22 mRNA and protein expression were detected by reverse transcription-PCR (RT-PCR) and Western blotting. The clones that had highest expression of IL-22 were picked and used in all experiments.

RT-PCR and real-time RT-PCR. Total cellular RNA was prepared using Trizol reagent and RT-PCR was done using the following set of primers: IL-22 (sense 5′-CACTGCAGGCTTGACAAG-3′ and antisense 5′-CTTAGCCTGTTGCTGAGC-3′), IL-22R1 (sense 5′-CCCCACTGGGACACTTTCTA-3′ and antisense 5′-TGGCCCTTTAGGTACTGTGG-3′), IL-10R2 (sense 5′-AGGGCTGAATTTGCAGATGA-3′ and antisense 5′-CCGTTTTTCCAGTATTGCAC-3′), and β-actin (sense 5′-GACCTGACTGACCACCTCATGAAGAT-3′ and antisense 5′-GTCACACTTCATGATGGAGTTGAAGG-3′). The PCR variables were 1 cycle at 95°C for 5 min then 30 cycles at 95°C for 30 s, 54°C for 30 s, and 72°C for 1 min followed by extension for 7 min at 72°C.

For real-time RT-PCR analysis, total cellular RNA was treated with DNase I (1 unit/μL; MBI Fermentas). Total RNA (1 μg) was reverse transcribed and quantified by TaqMan PCR on an ABI Prism 7000 Sequence Detection System (Applied Biosystems) with Premix Ex Taq Perfect Real-time Kit (TaKaRa). The set of primers and probes of human IL-22 gene and human β-actin gene were designed and synthesized by Invitrogen. All expression levels of target gene were normalized to the housekeeping gene β-actin (ΔCt). Gene expression values were then calculated based on the ΔΔCt method. Relative quantities (RQ) were determined using the equation: $RQ = 2^{\Delta\Delta Ct}$.

Protein isolation and Western blot assay. Cell pellets were resuspended in ice-cold NP-40 lysis buffer [50 mmol/L Tris-HCl (pH 6.8), 150 mmol/L NaCl, 1 mmol/L EGTA, and 1% NP-40] containing 1 mmol/L phenylmethylsulfonyl fluoride, 1 μg/mL leupeptin (Sigma), 1 μg/mL pepstatin (Sigma), and 1 μg/mL aprotinin (Sigma). The protein concentration was measured using Bio-Rad protein assay (Bio-Rad Laboratories). Protein extracts (60 μg) were subjected to electrophoresis on a 12% SDS-PAGE and electrophoretically transferred to nitrocellulose membranes. Membranes were blocked for 1 h with 5% nonfat dry milk in TBS containing 0.1% Tween 20 and successively incubated for 3 h with specific antibodies. After washing six times with TBS-Tween 20, the membranes were incubated for 1 h with horseradish peroxidase-conjugated secondary antibodies and visualized using an enhanced chemiluminescence detection system (SuperSignal West Dura Extended Duration Substrate; Pierce Chemical).

MTT assay. The MTT cell viability assay was done according to the manufacturer's instructions. Briefly, A549 and PG cells were washed with PBS and suspended in a final concentration of 2×10^5/mL in an assay medium. Cell suspension (10,000 cells; 100 μL) were dispensed

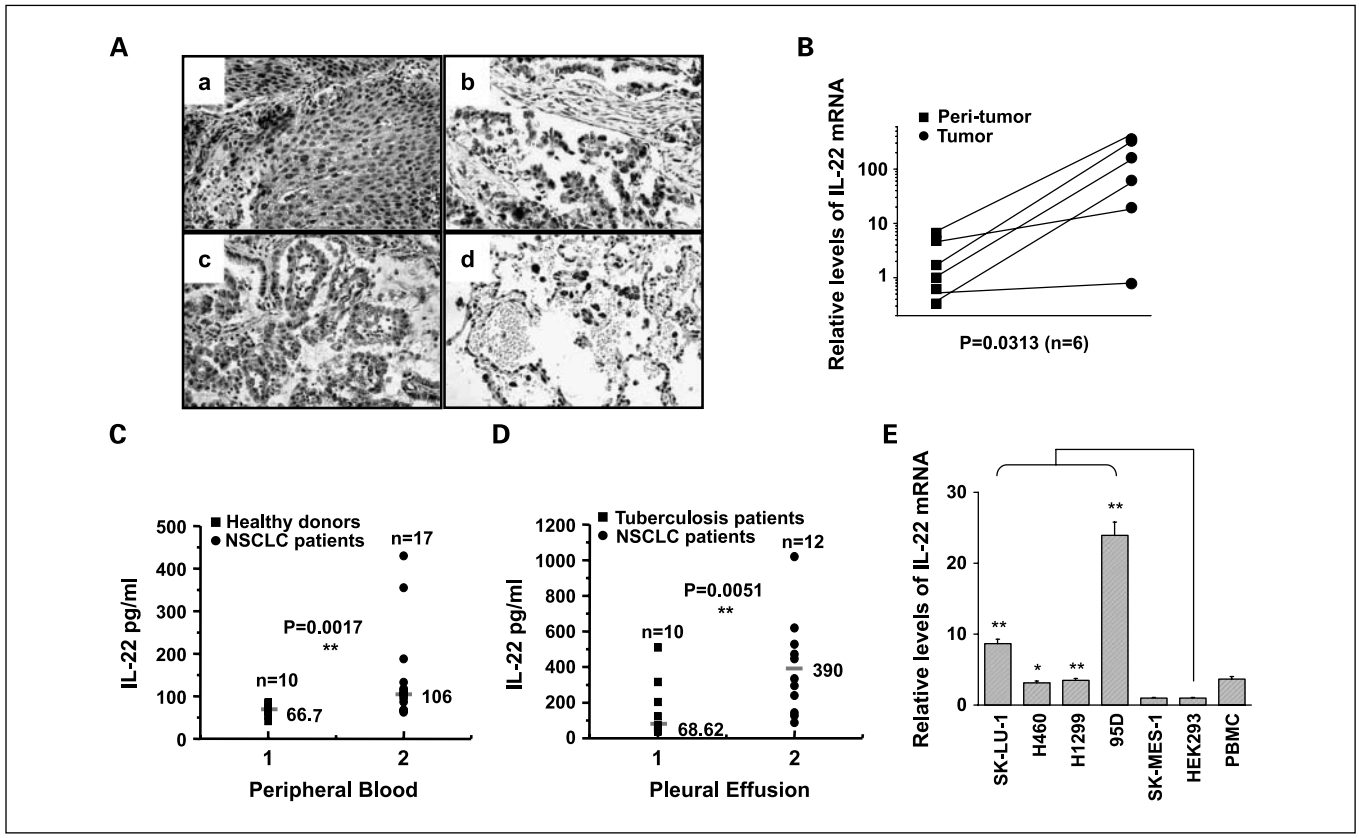

Fig. 1. IL-22 expression of clinical human NSCLC. *A,* immunohistochemical staining of human IL-22 in paraffin-embedded human lung cancer tissues showed cytoplasmic staining. IL-22 stainings were shown in representatives of squamous cell carcinoma (*a*), adenocarcinoma (*b* and *c*), and normal lung tissue control (*d*). *B,* paired lung cancer and peritumor lung specimens were obtained from the six surgical patients with a histologic diagnosis of NSCLC. IL-22 expression at the mRNA level was detected by real-time RT-PCR. All expression levels of target gene were normalized to the housekeeping gene β-actin (ΔCt). Gene expression values were then calculated based on the ΔΔCt method using the mean of one peritumor as calibrator. RQ was determined using the equation: $RQ = 2^{-\Delta\Delta Ct}$. *C,* peripheral blood was collected from healthy volunteers and patients with NSCLC and analyzed for serum IL-22 concentration by ELISA. **, $P < 0.01$, between the two groups. *D,* IL-22 levels in pleural fluid from NSCLC or tuberculosis patients were examined by ELISA; **, $P < 0.01$, between the two groups. *E,* real-time RT-PCR was used to detect the IL-22 mRNA expression. HEK293 was used as a normal cell control, whereas IL-2-stimulated PBMC served as a positive control. All expression levels of target gene were normalized to the housekeeping gene β-actin (ΔCt). Gene expression values were then calculated based on the ΔΔCt method using the mean of HEK293 as calibrator. RQ was determined using the equation: $RQ = 2^{-\Delta\Delta Ct}$. *, $P < 0.05$; **, $P < 0.01$.

into 96-well plates. The plates were incubated at 37°C for 48 h in a humidified CO_2 incubator. Complete culture medium (100 μL) with different concentrations of chemotherapeutic drug (0.005, 0.05, 0.5, and 5 mg/mL) were added into the wells and cultured for another 48 h. For the color development, 20 μL MTT (5 mg/mL) was added to each well and the plates were incubated at 37°C for 4 h, and 10% HCl-SDS (100 μL) was added to each well. The plates were kept at 4°C overnight, and using a 96-well plate reader, an absorbance rate at 570 nm wavelengths was recorded. Experiments were done in triplicate.

Annexin V/propidium iodide staining. Cells were seeded in six-well plates in a final concentration of 2×10^5/mL and induced by serum starvation or chemotherapeutic drug for indicated time. Cells were collected, washed with PBS, and successively resuspended in 100 μL binding buffer [10 mmol/L HEPES-NaOH (pH 7.4), 140 mmol/L NaCl, and 2.5 mmol/L $CaCl_2$]. Cells were incubated with 10 μL FITC-conjugated human Annexin V (BD Biosciences) in the dark for 30 min at 4°C and then stained with 5 μL propidium iodide (final concentration: 5 μg/mL). Ten minutes later, samples were immediately analyzed with a FACSCalibur (BD Biosciences).

Caspase activity assay. Caspase activity was detected using CaspSCREEN Flow Cytometric Apoptosis Detection Kit (BioVision). Briefly, 1×10^6 cells per well (2 mL) were seeded in a six-well plate the night before the treatment. Cells were treated with chemotherapeutic drug for the indicated times, collected, and washed with PBS twice. Cells (1×10^5) were resuspended in 0.3 mL D2R (aspartyl 2-rhodamine 110) incubation buffer. DTT (3 μL; 10 mmol/L final concentration) and D2R reagent (1 μL) were added. After 10 to 20 min incubation at 37°C in the dark, cells were analyzed by flow cytometry using FL-1 channel.

Transfection of IL-22-RNAi plasmid. The pU6+27 vector was used to express short hairpin RNA against IL-22. A 21-nucleotide sense and antisense hairpin oligonucleotide was generated complementary to IL-22 mRNA. Three RNAi sequences were designed, named IL-22-RNAi-1, IL-22-RNAi-2, and IL-22-RNAi03, in which the first nucleotide of RNAi corresponds to nucleotides 180, 378, and 438 of the IL-22 sequence, respectively. The top sequence of the IL-22-RNAi-1 (#1) was 5′-UCGACGGAGGCUAGCUUGGCUGAUUCAAGAGAUCAGCCAAGCUAGCCUCCUUUUUUU-3′, IL-22-RNAi-2 (#2) was 5′-UCGACCAGGCUAAGCACAUGUCAUUCAAGAGAUGACAUGUGCUUAGCCUGUUUUUUU-3′, and IL-22-RNAi-3 (#3) was 5′-UCGACGCUGAAGGACACAGUGAAAUUCAAGAGAUUUCACUGUGUCCUUCAGCUUUUUUU-3′. The sequence was inserted into the pU6+27 backbone after digestion with *Sal*I and *Xba*I. For plasmid transfection, cells were seeded at a density of 1×10^5 per well in a six-well plate. One day later, monolayer cells were subjected to transient transfection with IL-22-RNAi plasmid (#1, #2, or #3) or control plasmid using LipofectAMINE 2000 reagent (Invitrogen), respectively.

Mice and human lung cancer xenografts. A total of seven male BALB/c nude mice at age 6 weeks were used for the experiment. Xenograft tumor models were established as reported previously (14). A s.c. injection of 1×10^7 A549 cells into the flanks of mice was carried out.

Twenty-four hours later, the mice were randomly divided into two groups. The IL-22-RNAi group ($n = 4$) was injected i.v. with 50 μg IL-22-RNAi plasmid (#2) in 100 μL PBS followed by a booster of 25 μg plasmid in 100 μL PBS twice a week for a total of 6 weeks and 25 μg plasmid injected i.t. twice a week for a total of 3 weeks. The control group ($n = 3$) was injected with pU6+27 vector plasmid using the same protocol as the IL-22-RNAi group. Tumor formation was monitored daily and recorded. The studies have been reviewed and approved by an appropriate institutional review committee.

Statistical analysis. Statistical significance was determined if two-sided $P < 0.05$. Comparisons of cytokine concentrations between groups were done using the Mann-Whitney U test. Comparisons of IL-22 expression at mRNA levels between paired samples were done using the Wilcoxon matched-pairs signed-rank test. Student's t test was used to evaluate difference between individual groups.

Results

IL-22 is overexpressed in tumor tissue, malignant pleural effusion, and serum of human NSCLC. Previous studies have shown that IL-22 is a potential immunomodulatory molecule in the lung (13). To further investigate the role of IL-22 in NSCLC, 13 NSCLC specimens (7 adenocarcinomas and 6 squamous cell carcinomas) and normal lung samples were analyzed by immunohistochemistry. As shown in Fig. 1A, IL-22 staining in both adenocarcinoma and squamous cell carcinoma tumor cells was stronger than in normal alveolar epithelial cells. IL-22 mRNA expression in tumor tissues from patients with NSCLC was significantly higher than that in peritumor tissues by real-time RT-PCR analysis ($P = 0.0313$; Fig. 1B). IL-22 mRNA was also detected in 5 NSCLC cell lines and significantly higher in SK-LU-1, H460, H1299, and 95D NSCLC cell lines than that in normal control cell line HEK293 ($P < 0.01$, $P < 0.05$, $P < 0.01$, and $P < 0.01$, respectively; Fig. 1E). In addition, the median serum IL-22 content in NSCLC patients with stages I to III was significantly higher when compared with healthy individuals ($P = 0.0017$; Fig. 1C). Furthermore, when comparing malignant pleural effusion with tuberculous pleural effusion, IL-22 levels were increased sharply only in patients with stage IV NSCLC ($P = 0.0051$; Fig. 1D). Taken together, these results suggested that IL-22 was closely associated with human NSCLC.

Antiapoptosis by IL-22 overexpression in human lung cancer cells. Two human NSCLC cell lines, PG and A549, were chosen in our study based on the expression of IL-22 and IL-22 receptors. IL-22 receptor mRNA was detected in both A549 and PG cells, whereas IL-22 was only detected in A549 cells. To further investigate the effects of IL-22 in NSCLC, PG and A549 cells were stably transfected with the human IL-22 gene. As shown in Fig. 2A, the mRNA of IL-22 expression was much higher in IL-22-transfected PG cells (PG/IL-22) compared with PG control cells, whereas the expression of IL-22 moderately increased in IL-22-transfected A549 cells (A549/IL-22) compared with A549 control cells. The serum starvation-induced apoptosis of human cancer cells was done to test the antiapoptotic effect of IL-22. After serum starvation for 12 h, the percentage of cells in the early apoptotic stage (Annexin V-positive/propidium iodide-negative) was ~4-fold higher in PG/neo cells than that in PG/IL-22 cells (5.7 ± 1.2% versus 1.5 ± 0.6%, $P < 0.01$); also, a significant difference between A549/neo and A549/IL-22 was observed in the late apoptotic stage (Annexin V-positive/propidium iodide-positive) after 24 h of starvation (5 ± 1.1% versus 2.7 ± 0.6%; $P < 0.01$; Fig. 2B). Furthermore, the antiproliferative effects of chemotherapeutic drugs (5-FU or carboplatin) on cancer cells were suppressed both in IL-22 transgenic cell lines (Fig. 3A) and in the presence of recombinant human IL-22 (Fig. 3B). Additionally, the apoptosis-inducing effect of chemotherapeutic drugs on cancer cells was also inhibited in PG/IL-22 and A549/IL-22 cells (Fig. 3C and D). The number of cells in the late apoptotic stage was 12-fold higher in PG/neo cells and 3-fold higher in A549/neo cells when compared with IL-22-transfected cells in exposure to 5-FU (500 μg/mL) for 4 h (Fig. 3C).

Subsequently, we used IL-22R1 blocking antibodies to further confirm the role of IL-22 receptor signaling in chemotherapeutic drug resistance of NSCLC cell lines. As shown in Fig. 4, IL-22R1 blocking antibodies significantly promoted chemotherapeutic drug-induced apoptosis when compared with the isotype control. Because both IL-22 and

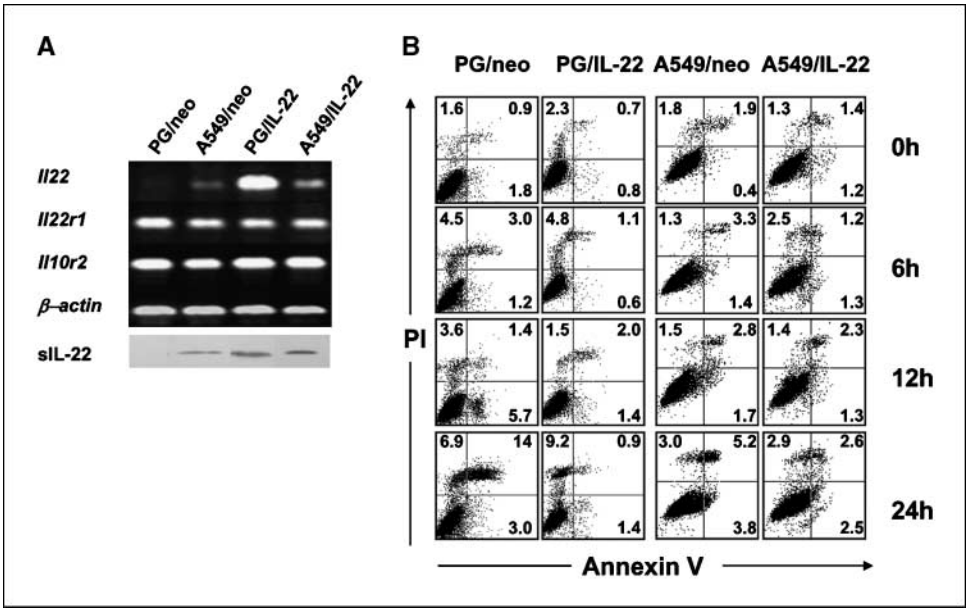

Fig. 2. IL-22 protects cancer cells from serum starvation-induced apoptosis. *A,* IL-22-transfected PG cells (PG/IL-22), IL-22-transfected A549 cells (A549/IL-22), and their control cells were subjected to RT-PCR. The supernatant was collected and analyzed for IL-22 by Western blotting. *B,* A549 and cells and their corresponding IL-22-transfected clones were plated in six-well plates at 2×10^5 to 5×10^5 per well and subjected to starvation with serum-free RPMI 1640 for various times. Cells were stained with Annexin V and propidium iodide to show the apoptosis. Representative of three independent experiments.

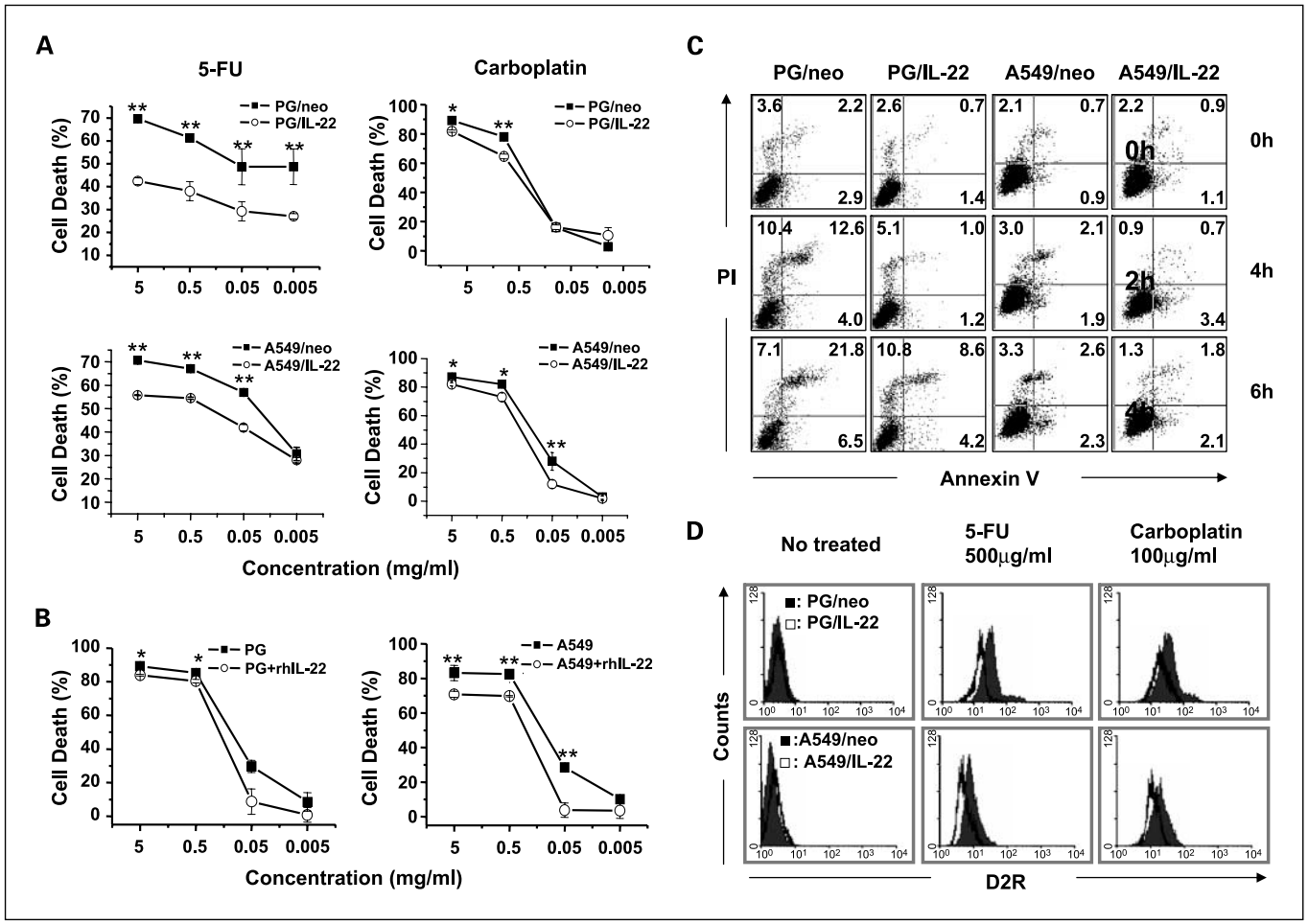

Fig. 3. IL-22 protects cancer cells from chemotherapeutic drug-induced apoptosis. *A,* PG/IL-22, A549/IL-22, and their control cells (2×10^4) were cultured in 96-well plates and exposed to 5-FU or carboplatin at different final concentrations (5, 0.5, 0.05, and 0.005 mg/mL) for 48 h. The cell death rate was evaluated by MTT assay. *B,* 2×10^4 A549 and PG cells were exposed to carboplatin at different final concentrations in the presence or absence of human recombinant IL-22 (20 ng/mL) for 48 h. The cell death rate was evaluated by MTT assay. *C,* 2×10^5 cells were cultured in six-well plates overnight and then exposed to 5-FU (500 μg/mL). Cells were harvested at indicated time points and stained with Annexin V/propidium iodide for fluorescence-activated cell sorting analysis. *D,* 5-FU or carboplatin was used to induce cell apoptosis at a final concentration of 500 or 100 μg/mL, respectively. Exposing cancer cells to chemotherapeutic drug for 8 h, apoptotic cells were evaluated using CaspSCREEN Caspase Screening Kit. Mean ± SD of three independent experiments. *, $P < 0.05$; **, $P < 0.01$.

its functional receptor complex were detected in the A549 cell line (Fig. 2A) in the absence of the IL-22 transgene, anti-IL-22R1 antibodies increased apoptotic effects of 5-FU on A549/neo cells (Fig. 4). Because no constitutive expression of IL-22 was found in PG/neo cells, the blocking antibody against IL-22 receptor had no effect on drug-induced apoptosis in this IL-22-negative cancer cell line (Fig. 4). This suggested that the antiapoptotic effect of IL-22 was mediated by the interaction between IL-22 and its functional receptor complex.

Antiapoptotic effects of IL-22 in human lung cancer cells is via STAT3 and ERK1/2 pathways. It was noted that STAT3 was constitutively activated with high frequency in tumor and critical in promoting tumor cell growth and survival. We found that the antiapoptotic effect of IL-22 in PG cells (PG/IL-22 cells) but not A549/IL-22 cells was closely correlated to STAT3 activation, as STAT3 phosphorylation in PG/IL-22 cells was much higher than that in PG/neo cells (Fig. 5A). Meanwhile, the antiapoptotic proteins (Bcl-xL and Bcl-2) were consistently induced in PG/IL-22 cells regardless of 5-FU treatment, whose levels were higher than that in PG/neo cells (Fig. 5B and C). However, IL-22 transfection into A549 cells (A549/IL-22) did not so dramatically increase the activation of STAT3 (Fig. 5A and B) and production of Bcl-xL and Bcl-2 (Fig. 5B) as it did in PG cells, which is accordance with the observation that A549/neo cells were more resistant to apoptosis than PG/neo cells after serum starvation (Fig. 2B) or 5-FU treatment (Fig. 3C) by constitutively higher IL-22 autoproduction in A549/neo cells (Fig. 2A). On the other hand, it was obviously observed that IL-22 overexpression in PG and A549 cells inhibited phosphorylation of ERK1/2 (Fig. 5A). Therefore, to verify the IL-22 effects on A549 cells, IL-22-mRNAi was examined. As shown in Fig. 6C and D and Supplementary Fig. S1, IL-22-RNAi induced phosphorylation of ERK1/2 as well as inhibited the activation of STAT3 but did not induce the AKT activation in A549 cells. Taken together, these results suggested that antiapoptotic effects of IL-22 were possibly correlated to the inactivation of ERK1/2, activation of STAT3, and then induction of Bcl-2/Bcl-xL.

Therapeutic effects of IL-22-small interfering RNA by inducing apoptosis on human lung cancer xenografts. To assess whether IL-22 affects cell survival, three different plasmids of IL-22-RNAi were designed and transfected into A549 cells, which

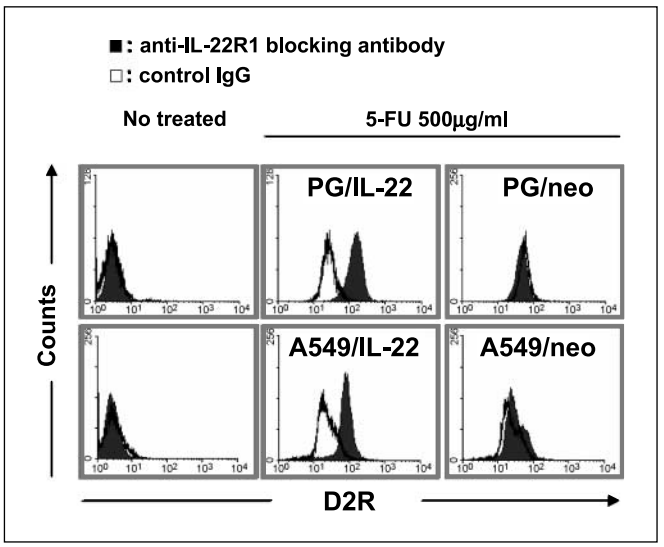

Fig. 4. IL-22 mediates antiapoptotic activity via its receptor. PG/IL-22, A549/IL-22, and their control cells (2×10^5) were cultured in six-well plates overnight and then treated with IL-22R1 blocking antibody at a final concentration of 2 μg/mL. The normal goat IgG served as a negative control. After 30 min, chemotherapeutic drug (5-FU) was added at a final concentration of 500 μg/mL. Eight hours later, apoptotic cells were evaluated using CaspSCREEN Caspase Screening Kit.

constitutively express higher level of autocrine IL-22. Forty-eight hours after IL-22-RNAi vector transfection into A549 cells, IL-22 protein synthesis was almost completely blocked (Fig. 6A). The most effective IL-22-RNAi vector (#2) was then used. Meanwhile, inhibition of IL-22 expression by RNAi caused a significant increase in apoptosis of A549 cells induced by chemotherapeutic drugs (Fig. 6B) but not in a human normal endothelial cell line (HUV-EC-C cells; Supplementary Fig. S2). Furthermore, our results revealed that IL-22-RNAi inhibited the activation of STAT3 (Fig. 6C) and induced phosphorylation of ERK1/2 (Fig. 6C and D) but did not induce the AKT activation (Supplementary Fig. S1).

Subsequently, we established xenograft tumors in BALB/c nude mice to analyze the effects of IL-22 RNAi on tumor cell growth *in vivo*. Cancer cells (1×10^7) were injected s.c. into the lower right flank of nude mice. IL-22 RNAi plasmids or control plasmids were administrated into mice according to the schedule shown in Fig. 6E. The relative tumor growth of xenografted mice was monitored for 38 days with termination at 59 days post-inoculation. Tumor volume was significantly lower in IL-22-RNAi-treated mice than that in vector control mice ($P < 0.01$; Fig. 6F). Tumor weight was also significantly decreased in IL-22-RNAi-treated mice (data not shown).

Discussion

In this study, we first showed that IL-22 was overexpressed in primary tumor tissue, malignant pleural effusion, and serum in patients with NSCLC and that the overexpression of IL-22 was possibly correlated with occurrence and progress of human NSCLC. Furthermore, the fact that gene silencing of IL-22 by small interfering RNA significantly inhibited xenograft tumor growth suggested that IL-22 played an important role in NSCLC progression.

Reports relating to the association of IL-22 expression with tumor growth and apoptosis are few and varied. Although the growth of IL-22-transfected colon 26 cells was not different from that of control cells *in vitro*, survival of inoculated mice was significantly prolonged compared with control mice, suggesting that IL-22 might play a protective role in the mice with colon carcinoma (15). In contrast, Weber et al. (16) reported that IL-22 reduced EMT6 murine breast tumor growth by inhibiting ERK1/2 and AKT phosphorylation. On the other hand, in an *in vitro* study using HepG2 human hepatocellular carcinoma cells, it was noted that IL-22 transfection promoted cell growth and survival by activation of STAT3 and induction of antiapoptotic and mitogenic proteins (10). In addition, it was reported that isochaihulactone induced apoptosis in A549 cells via the phosphorylation of ERK1/2 but not on the activation of protein kinase C or AKT/glycogen synthase kinase-3β (17). FOH-induced apoptosis in

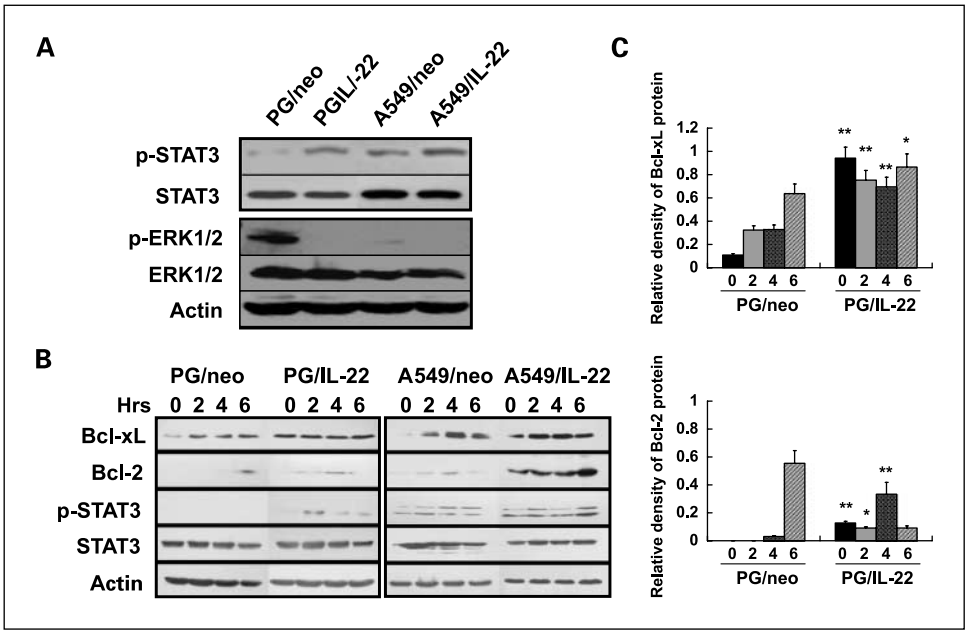

Fig. 5. Antiapoptotic proteins Bcl-2 and Bcl-xL are induced via the activation of STAT3 by IL-22 stimulation. *A,* PG/IL-22, A549/IL-22, and their control cells were cultured in complete RPMI 1640 for 48 h. Equal amounts of cell lysates were subjected to SDS-PAGE and Western blotting using anti-STAT3, anti-phosphorylated STAT3, anti-ERK1/2, anti-phosphorylated ERK1/2 (Thr^{202}/Tyr^{204}), and anti-β-actin antibodies. *B,* cells were treated with 5-FU (500 μg/mL, final concentration) and harvested at the indicated time points (h). Western blotting was done to detect the activation of STAT3 and induction of subsequent antiapoptotic proteins Bcl-xL and Bcl-2. *C,* bands in Fig. 5B were then analyzed by Scion Image software for the relative density compared with β-actin. *, $P < 0.05$; **, $P < 0.01$, compared with corresponding control.

human lung carcinoma cells was dependent on the activation of the MEK-ERK signaling pathway (18), and PG490 (triptolide)-mediated sensitization of human lung cancer cells to Apo2L/TRAIL-induced apoptosis required activation of ERK2 (19). In the current study, both *in vitro* and *in vivo* data showed that overexpression of IL-22 protected lung cancer cells from apoptosis (Figs. 1–3 and 6) via the activation of STAT3 and its downstream antiapoptotic proteins such as Bcl-2 and Bcl-xL and inactivation of ERK1/2 (Fig. 5). Our results (Fig. 6C and D; Supplementary Fig. S1) also suggested that the activation of ERK1/2 and inactivation of STAT3, but not AKT pathway, were involved in the antitumor effect of IL-22-RNAi in A549 cells.

The conflicting data produced by various investigators may be due to differences in disease models, species, and cell types studies as well as the pleiotropic roles of IL-22. In our study, A549 cells, one of most extensively used NSCLC models, were selected based on the clinical observation that overproduction of IL-22 was correlated with progression of NSCLC (Fig. 1). Furthermore, it has been shown that NSCLC possess several intracellular signaling pathways that act against chemotherapeutic insults including the anticancer drug-induced or constitutive activation of the phosphatidylinositide 3-kinase (20), the nuclear factor-κB, Akt (21–24), and the STAT3 signaling pathways (25). In our study, an increase in both constitutive and chemotherapeutic drug-induced activation of STAT3 was detected in A549 cells (Fig. 5). In addition, inhibition of IL-22 could enhance the sensitivity of A549 cells to chemotherapeutic drugs (Fig. 6B). Hence, IL-22 contributed to the activation of STAT3 and chemoresistant effect in NSCLC cells.

Autocrine production of cytokines is required for cell survival and growth and is responsible for resistance to apoptosis induced by antitumor drugs in many cancer cells. It has been shown that autocrine IL-4 and IL-10 production in thyroid cancer cells results in constitutive activation of the JAK/STAT pathway that protects cells against CD95-induced (26) and chemotherapeutic drug-induced apoptosis (27). Moreover, autocrine IL-6-induced STAT3 activation contributes to the pathogenesis of lung adenocarcinoma and formation of malignant pleural effusion (25). Similar to these findings, we found that there was an autocrine IL-22 production in NSCLC. The constitutive production of IL-22 was observed in primary NSCLC (Fig. 1) and A549 cells (Fig. 2). Other researchers (13, 28) and our studies (Fig. 2) showed that functional IL-22 receptor complex was detected in A549 cells. Blocking this functional IL-22 autocrine loop using anti-IL-22R1 Abs resulted in an increased chemotherapeutic drug-induced apoptosis in A549 cells (Fig. 4). These results, for the first time, provided evidence that IL-22 can directly act on NSCLC cells by increasing the expression of antiapoptotic proteins, thus promoting the resistance of NSCLC cells to antitumor drugs.

It is well known that development of malignant pleural effusion is associated with a poor prognosis. In malignant pleural effusions, the mRNA expressions of IL-4, IL-10, tumor necrosis factor-α, and transforming growth factor-β1 were significantly higher than those from tuberculosis pleural effusion (29). Higher levels of IL-6 (25) and VEGF (25, 30) were also found in the pleural fluids of patients with NSCLC and contributed to the formation of malignant pleural effusion.

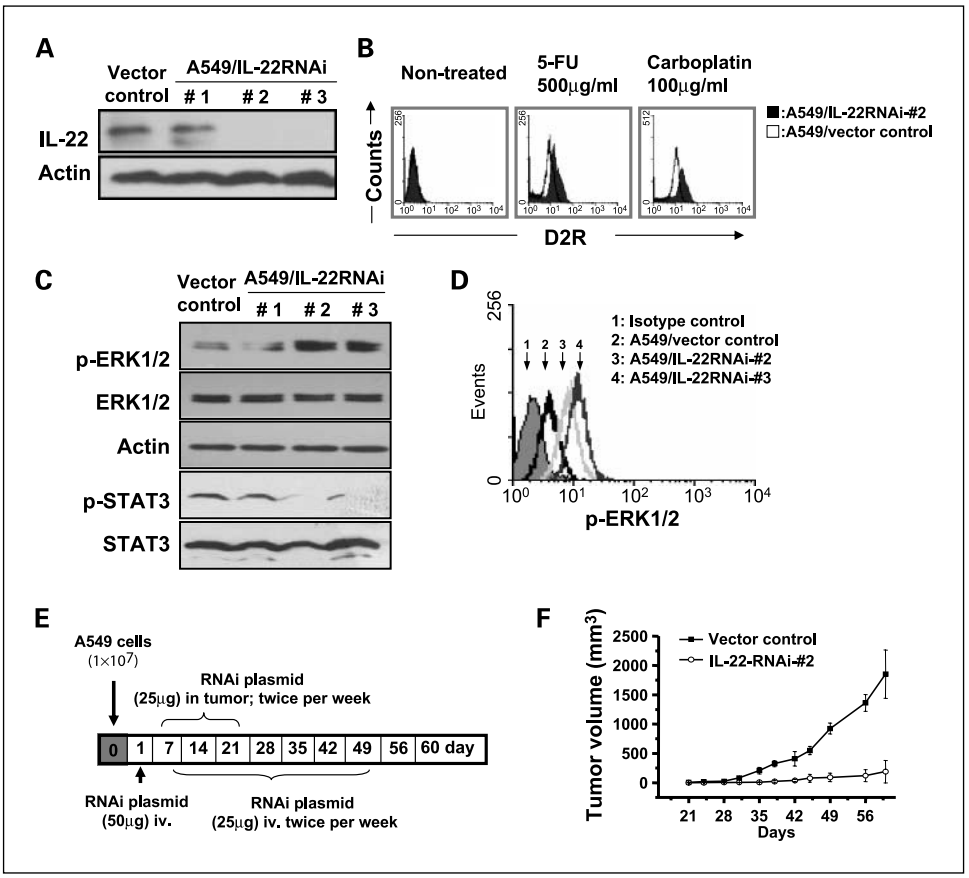

Fig. 6. Therapeutic effects of IL-22-RNAi plasmid in tumor xenograft BALB/c-*nu/nu* mice. *A,* three different plasmids of IL-22-RNAi were designed and transient transfected into A549 cells by LipofectAMINE 2000. Forty-eight hours after transfection, examination of IL-22 protein in IL-22-RNAi transiently transfected A549 cells was done by Western blotting to screen the most effective plasmid of IL-22-RNAi. *B,* A549 cells (2×10^5) in six-well plate were transient transfected with IL-22-RNAi plasmid (#2) or control vector and cultured for 48 h followed by exposure to chemotherapeutic drugs for 8 h. The cells were finally examined for apoptosis by CaspSCREEN Caspase Screening Kit. *C* and *D,* A549 cells were plated in six-well plates at 1×10^5 per well. One day later, monolayer cells were subjected to transient transfection with IL-22-RNAi by LipofectAMINE 2000. At 48 h after transfection, Western blotting analysis (*C*) and flow cytometry analysis (*D*) were done to determine the phosphorylation of ERK1/2 and STAT3. Representative of three independent experiments. *E,* schematic diagram of injection protocols for IL-22-RNAi plasmids. A549 cells suspended in 100 μL PBS was s.c. inoculated in the right flank of nude mice. On the next day, 50 μg IL-22-RNAi plasmid (#2; $n = 4$) or control plasmid ($n = 3$) in a total of 100 μL PBS was injected i.v. followed by treatment with 25 μg plasmid i.v. (totally injected for 12 times) and i.t. (totally injected for 6 times) twice a week. *F,* tumor growth was monitored and recorded from days 21 to 59. Tumor volume was calculated as length × width × height.

Our current data showed that the significantly elevated expression of IL-22 in malignant pleural effusion might serve as the antiapoptotic factor responsible for cancer cell survival (Fig. 1D). Although the role of autocrine production of IL-22 needs further study, our *in vitro* and *in vivo* observations suggest that this cytokine may possibly be a novel target for diagnosis, treatment, and prognosis of NSCLC.

Disclosure of Potential Conflicts of Interest

No potential conflicts of interest were disclosed.

Acknowledgments

We thank Xin-yu Mei, Xian-li Guo, and Hui-ning Liu for sampling assistance.

References

1. Volm M, Rittgen W. Cellular predictive factors for the drug response of lung cancer. Anticancer Res 2000; 20:3449–58.
2. Gallego MA, Joseph B, Hemstrom TH, et al. Apoptosis-inducing factor determines the chemoresistance of non-small-cell lung carcinomas. Oncogene 2004;23: 6282–91.
3. Berman KS, Verma UN, Harburg G, Minna JD, Cobb MH, Gaynor RB. Sulindac enhances tumor necrosis factor-α-mediated apoptosis of lung cancer cell lines by inhibition of nuclear factor-κB. Clin Cancer Res 2002;8:354–60.
4. Jones DR, Broad RM, Comeau LD, Parsons SJ, Mayo MW. Inhibition of nuclear factor κB chemosensitizes non-small cell lung cancer through cytochrome *c* release and caspase activation. J Thorac Cardiovasc Surg 2002;123:310–7.
5. Dumoutier L, Louahed J, Renauld JC. Cloning and characterization of IL-10-related T cell-derived inducible factor (IL-TIF), a novel cytokine structurally related to IL-10 and inducible by IL-9. J Immunol 2000;164: 1814–9.
6. Pestka S, Krause CD, Sarkar D, Walter MR, Shi Y, Fisher PB. Interleukin-10 and related cytokines and receptors. Annu Rev Immunol 2004;22:929–79.
7. Kotenko SV, Izotova LS, Mirochnitchenko OV, et al. Identification of the functional interleukin-22 (IL-22) receptor complex: the IL-10R2 chain (IL-10Rβ) is a common chain of both the IL-10 and IL-22 (IL-10-related T cell-derived inducible factor, IL-TIF) receptor complexes. J Biol Chem 2001;276: 2725–32.
8. Xie MH, Aggarwal S, Ho WH, et al. Interleukin (IL)-22, a novel human cytokine that signals through the interferon receptor-related proteins CRF2-4 and IL-22R. J Biol Chem 2000;275:31335–9.
9. Lejeune D, Dumoutier L, Constantinescu S, Kruijer W, Schuringa JJ, Renauld JC. Interleukin-22 (IL-22) activates the JAK/STAT, ERK, JNK, and p38 MAP kinase pathways in a rat hepatoma cell line. Pathways that are shared with and distinct from IL-10. J Biol Chem 2002;277:33676–82.
10. Radaeva S, Sun R, Pan HN, Hong F, Gao B. Interleukin 22 (IL-22) plays a protective role in T cell-mediated murine hepatitis: IL-22 is a survival factor for hepatocytes via STAT3 activation. Hepatology 2004;39: 1332–42.
11. Pan H, Hong F, Radaeva S, Gao B. Hydrodynamic gene delivery of interleukin-22 protects the mouse liver rom concanavalin A-, carbon tetrachloride-, and Fas ligand-induced injury via activation of STAT3. Cell Mol Immunol 2004;1:43–9.
12. Brand S, Dambacher J, Beigel F, et al. IL-22-mediated liver cell regeneration is abrogated by SOCS-1/3 overexpression *in vitro*. Am J Physiol Gastrointest Liver Physiol 2007;292:G1019–28.
13. Whittington HA, Armstrong L, Uppington KM, Millar AB. Interleukin-22: a potential immunomodulatory molecule in the lung. Am J Respir Cell Mol Biol 2004; 31:220–6.
14. Chen YJ, Chang JT, Lee L, et al. DSG3 is overexpressed in head neck cancer and is a potential molecular target for inhibition of oncogenesis. Oncogene 2007;26:467–76.
15. Nagakawa H, Shimozato O, Yu L, et al. Expression of interleukin-22 in murine carcinoma cells did not influence tumour growth *in vivo* but did improve survival of the inoculated hosts. Scand J Immunol 2004;60: 449–54.
16. Weber GF, Gaertner FC, Erl W, et al. IL-22-mediated tumor growth reduction correlates with inhibition of ERK1/2 and AKT phosphorylation and induction of cell cycle arrest in the G_2-M phase. J Immunol 2006; 177:8266–72.
17. Chen YL, Lin PC, Chen SP, et al. Activation of nonsteroidal anti-inflammatory drug-activated gene-1 via extracellular signal-regulated kinase 1/2 mitogen-activated protein kinase revealed a isochaihulactone-triggered apoptotic pathway in human lung cancer A549 cells. J Pharmacol Exp Ther 2007;323:746–56.
18. Joo JH, Liao G, Collins JB, Grissom SF, Jetten AM. Farnesol-induced apoptosis in human lung carcinoma cells is coupled to the endoplasmic reticulum stress response. Cancer Res 2007;67:7929–36.
19. Frese S, Pirnia F, Miescher D, et al. PG490-mediated sensitization of lung cancer cells to Apo2L/TRAIL-induced apoptosis requires activation of ERK2. Oncogene 2003;22:5427–35.
20. Lee HY, Srinivas H, Xia D, et al. Evidence that phosphatidylinositol 3-kinase- and mitogen-activated protein kinase kinase-4/c-Jun NH_2-terminal kinase-dependent pathways cooperate to maintain lung cancer cell survival. J Biol Chem 2003;278:23630–8.
21. Sun C, Chan F, Briassouli P, Linardopoulos S. Aurora kinase inhibition downregulates NF-κB and sensitises tumour cells to chemotherapeutic agents. Biochem Biophys Res Commun 2007;352:220–5.
22. Singh RP, Mallikarjuna GU, Sharma G, et al. Oral silibinin inhibits lung tumor growth in athymic nude mice and forms a novel chemocombination with doxorubicin targeting nuclear factor κB-mediated inducible chemoresistance. Clin Cancer Res 2004;10:8641–7.
23. Mayo MW, Denlinger CE, Broad RM, et al. Ineffectiveness of histone deacetylase inhibitors to induce apoptosis involves the transcriptional activation of NF-κB through the Akt pathway. J Biol Chem 2003; 278:18980–9.
24. Mijatovic T, Op De Beeck A, Van Quaquebeke E, et al. The cardenolide UNBS1450 is able to deactivate nuclear factor κB-mediated cytoprotective effects in human non-small cell lung cancer cells. Mol Cancer Ther 2006;5:391–9.
25. Yeh HH, Lai WW, Chen HH, Liu HS, Su WC. Autocrine IL-6-induced Stat3 activation contributes to the pathogenesis of lung adenocarcinoma and malignant pleural effusion. Oncogene 2006;25:4300–9.
26. Todaro M, Zerilli M, Ricci-Vitiani L, et al. Autocrine production of interleukin-4 and interleukin-10 is required for survival and growth of thyroid cancer cells. Cancer Res 2006;66:1491–9.
27. Stassi G, Todaro M, Zerilli M, et al. Thyroid cancer resistance to chemotherapeutic drugs via autocrine production of interleukin-4 and interleukin-10. Cancer Res 2003;63:6784–90.
28. Wolk K, Kunz S, Witte E, Friedrich M, Asadullah K, Sabat R. IL-22 increases the innate immunity of tissues. Immunity 2004;21:241–54.
29. Li R, Ruttinger D, Li R, Si LS, Wang YL. Analysis of the immunological microenvironment at the tumor site in patients with non-small cell lung cancer. Langenbecks Arch Surg 2003;388:406–12.
30. Zebrowski BK, Yano S, Liu W, et al. Vascular endothelial growth factor levels and induction of permeability in malignant pleural effusions. Clin Cancer Res 1999;5:3364–8.

Clinical Cancer Research

Antiapoptotic Activity of Autocrine Interleukin-22 and Therapeutic Effects of Interleukin-22-Small Interfering RNA on Human Lung Cancer Xenografts

Weici Zhang, Yongyan Chen, Haiming Wei, et al.

Clin Cancer Res 2008;14:6432-6439.